

# Journal of Materials Chemistry B

Accepted Manuscript



This is an *Accepted Manuscript*, which has been through the Royal Society of Chemistry peer review process and has been accepted for publication.

*Accepted Manuscripts* are published online shortly after acceptance, before technical editing, formatting and proof reading. Using this free service, authors can make their results available to the community, in citable form, before we publish the edited article. We will replace this *Accepted Manuscript* with the edited and formatted *Advance Article* as soon as it is available.

You can find more information about *Accepted Manuscripts* in the [Information for Authors](#).

Please note that technical editing may introduce minor changes to the text and/or graphics, which may alter content. The journal's standard [Terms & Conditions](#) and the [Ethical guidelines](#) still apply. In no event shall the Royal Society of Chemistry be held responsible for any errors or omissions in this *Accepted Manuscript* or any consequences arising from the use of any information it contains.

Cite this: DOI: 10.1039/c0xx00000x

www.rsc.org/xxxxxx

ARTICLE TYPE

# Mussel-inspired chitooligosaccharide based multidentate ligand for highly stabilized nanoparticles

Chichong Lu,<sup>\*a</sup> Min Kyu Park,<sup>b</sup> Chenxin Lu,<sup>c</sup> Young Haeng Lee,<sup>b</sup> and Kyu Yun Chai<sup>\*b</sup>

Received (in XXX, XXX) Xth XXXXXXXXX 20XX, Accepted Xth XXXXXXXXX 20XX

DOI: 10.1039/b000000x

Inspired by the adhesion behaviors of mussels, we synthesized a chitooligosaccharide (COS) based multidentate ligand (ML) for preparing robust biocompatible magnetic iron oxide nanoparticles (IONPs). The COS was modified with mussel adhesive proteins (MAPs) mimetic multiple catechol groups and branched poly(ethylene glycol) moieties, which can not only strongly bind to IONPs through multiple catechol groups, but also afford IONPs with good colloidal stability and biocompatibility due to PEG integrated into the COS coating. The resultant ML-stabilized IONPs consist of single nanoparticles coated with ML shells and exhibited high dispersion stability in aqueous solution for a wide range of pH and concentrated salt solutions. The potential of ML-stabilized IONPs as contrast agents for  $T_2$ -weighted magnetic resonance imaging was demonstrated by conducting *in vivo* imaging and relaxivity measurements. The ML-stabilized IONPs are therefore expected to be useful for magnetic resonance imaging under physiological conditions.

## Introduction

Colloidal nanoparticles have been extensively used in the biomedical diagnostic and therapeutic fields owing to their useful optical, electronic, and magnetic properties.<sup>1-4</sup> In particular, iron oxide nanoparticles (IONPs) have been extensively studied due to their unique magnetic properties and low toxicity.<sup>5-9</sup> Successful *in vivo* usage of IONPs requires particles below 100 nm in size that are well dispersed in the physiological media. Unfortunately, bare IONPs are not stable in water or in physiological fluids. To ensure the stability of IONPs and to promote their dispersion in aqueous media, there are two common coating strategies to convert hydrophobic ones into hydrophilic and functional nanoparticles. The first approach involves the ligand exchange of the original surfactant by hydrophilic ligands such as carboxylic acids, phosphonates, thiols, and organosilanes, which form strong coordinative bonds with metal oxide nanoparticles.<sup>10-15</sup> The second approach is to encapsulate the nanoparticles with amphiphilic polymers in a micelle format.<sup>16-19</sup>

In contrast to these surface-specific interactions, marine mussels (e.g., *Mytilus edulis*) are known to adhere onto various substrates.<sup>20-24</sup> An unusual amino acid, 3,4-dihydroxy-L-phenylalanine (DOPA), is abundant in mussel adhesive proteins (MAPs) secreted at the interface between adhesive pads and opposing surfaces. The *ortho*-dihydroxyphenyl (catechol) functional group is believed to be responsible for the adhesive characteristics of MAPs, which play an important role as surface-independent anchor molecules for the modification of nanoparticles.<sup>25-30</sup> More importantly, for the biofunctionalization of the nanoparticles, a binding site can be provided for other bioactive molecules that can further extend the biomedical

applications. One such molecule is chitosan, which is a linear nontoxic biocompatible and biodegradable polymer. It has been hypothesized that chitosan directly interacts with cell membranes,<sup>31</sup> which may facilitate the uptake of chitosan-coated IONPs by the stem cells. Such characteristics make them are of interest in the development of iron oxide-chitosan nanoparticles. However, the solubility and colloidal stability of such particles in aqueous media have not been previously addressed or optimized. In addition, such particles were polydisperse and consist of agglomerated cores of primary particles, since the chitosan is adsorbed to the surface of the particle rather than chemically bound, and because of the large molecular weight.<sup>32-36</sup> Chitooligosaccharide (COS), which are entirely biodegradable and highly water-soluble oligosaccharide made from chitosan by chemical or enzymatic decomposing methods, was widely employed in the drug/gene delivery systems. Rinaldi *et al*<sup>37</sup> developed magnetic nanoparticles consisting of iron oxide cores modified with covalently linked COS that were colloiddally stable in water and buffers. Hyeon *et al*<sup>38</sup> developed COS-stabilized ferrimagnetic iron oxide nanocubes as an effective heat nanomediator for cancer hyperthermia. Ji *et al*<sup>39</sup> demonstrated a multidentate dithiolane lipoic acid and phosphorylcholine conjugated COS derivative that can serve as a ligand to effectively stabilize gold nanoparticles. Also, chitosan and COS molecules have no amphiphilic property and cannot be directly used to stabilize hydrophobic nanoparticles. Therefore, it should be modified firstly to facilitate its solubility in organic solvent such as chloroform. With regard to the biofunctionalization of IONPs, polyethylene glycol (PEG), one of the most popular amphiphilic polymer modifiers, is widely used, partly because of its biocompatibility and anti-biofouling properties, which prevent

adsorption of plasma proteins or cells onto nanoparticle surfaces, thereby increasing the blood circulation time and allowing the nanoparticles to reach their target tissues. These observations point toward the possibility of synthesizing PEG and catechol functionalized COS as a ligand for preparing robust biocompatible magnetic IONPs. Inspired by mussels, catechol-derived multidentate ligands have also been utilized as high-affinity anchors for nanoparticle stabilization.<sup>40-45</sup> Herein, we report the design and synthesis of a COS based multidentate ligand (ML) for ultrastable and biocompatible nanoparticles. To the best of our knowledge, this is the first report on the PEG-g-COS based multidentate ligand for water-dispersible magnetic IONPs. Poly(ethylene glycol) methyl ether (mPEG) was grafted onto COS not only to render amphiphilic and ultrastable with respect to aggregation, but also to impart anti-biofouling properties. Scheme 1 shows the design and synthesis of ML, which has a branched architecture, mPEG-g-COS as a scaffold and multiple catechol unit domains for multivalent anchoring. The amine groups present on the COS scaffold were covalently bound to mPEG, 28% of them were further functionalized by catecholic groups. The remaining amine groups afforded more functional groups for secondary modifications of the ligand. The ML coating protocol for nanoparticles was very simple and did not disturb the crystal structure. Stabilities, cytotoxicity and biocompatibility of ML-stabilized IONPs were evaluated, which promises good properties of this IONPs formulation for *in vivo* magnetic resonance imaging (MRI) application.

## Experimental

**Materials.** Chitooligosaccharide (COS,  $M_w = 3000$  Da, deacetylation degree = 92%) was purchased from Chittolife Co., Ltd. (Seoul, Korea). Hydrocaffeic acid (HCA, 3,4-dihydroxy hydrocinnamic acid), poly(ethylene glycol) methyl ether (mPEG-OH,  $M_n = 2000$  Da), 1-ethyl-3-(3-dimethylaminopropyl)-carbodiimide hydrochloride (EDC), *N*-hydroxysuccinimide (NHS), dichloromethane (DCM), and chloroform were purchased from Sigma-Aldrich. All the other chemicals were of analytical grade.

### Synthesis of mPEG-COOH

A solution of mPEG-OH (6 mmol,  $M_n = 2000$ ) and potassium hydroxide (0.4 g, 7 mol) in distilled water (15.0 g) was stirred for 30 min in an ice bath. Acrylonitrile (0.5 g, 9.42 mmol) was added slowly, and the solution was stirred for 2 hours at 0–5 °C. Concentrated sulfuric acid (30.0 g) was added, and the mixture was heated for 3 hours at 95–100 °C. After the mixture was cooled to room temperature, distilled water (200 mL) was added, and the reaction products were extracted with DCM (3 × 30 mL). The extract was dried with anhydrous sodium sulfate, and the solvent was distilled off under reduced pressure. Pure mPEG-COOH was separated by ion exchange chromatography on DEAE-Sephadex A-25. <sup>1</sup>H NMR (500 MHz, CDCl<sub>3</sub>): δ 3.7–3.5 (m, PEG backbone), 3.3 (s, 3H, CH<sub>3</sub>-O-), 2.5 (t, 2H,  $J = 6.0$  Hz, -CH<sub>2</sub>-C(O)O-).

### Synthesis of mPEG-grafted COS (mPEG-g-COS)

In brief, COS (0.5 g, 3 mmol of monomers) was dissolved in 30 mL of deionized water. mPEG-COOH (1.87 g, 0.9 mmol) and

NHS (0.5 g, 4.5 mmol) were added to the solution. Then, EDC (0.86 g, 4.5 mmol) was added in small portions. The resulting solution was stirred at room temperature for 24 h and subsequently purified by dialysis (Mw cutoff of 12 kDa) against deionized water for 2 days, followed by lyophilization. <sup>1</sup>H NMR (500 MHz, CDCl<sub>3</sub>): δ 3.5–4.0 (m, H-3, H-4, H-5, H-6 of COS and PEG backbone), 3.3 (s, 3H, CH<sub>3</sub>-O-), 2.5 (t, 2H,  $J = 6.0$  Hz, -CH<sub>2</sub>-C(O)O-), 2.0 (br s, NHAc).

### Synthesis of ML

The ML was synthesized by conjugating a carboxylic acid group of hydrocaffeic acid to an amine group of COS backbone and initiated from mPEG-g-COS using carbodiimide chemistry.<sup>45,46</sup> In brief, EDC (0.13 g, 0.68 mmol) dissolved in 5 mL of methanol was slowly added to a stirred solution of 2 mL of anhydrous dimethylformamide (DMF) containing hydrocaffeic acid (0.06 g, 0.34 mmol). The activated hydrocaffeic acid was then reacted with 0.54 g of mPEG-g-COS dissolved in 5 mL of methanol for 24 h under nitrogen atmosphere. The solution was precipitated into excess cold ethyl ether, and the residual solvent was removed under vacuum. The polymer was purified by dialysis against acidified deionized water for 2 days (Mw cutoff of 12 kDa), and then lyophilized.

### Preparation of the ML-stabilized water-soluble IONPs (ML-IONPs)

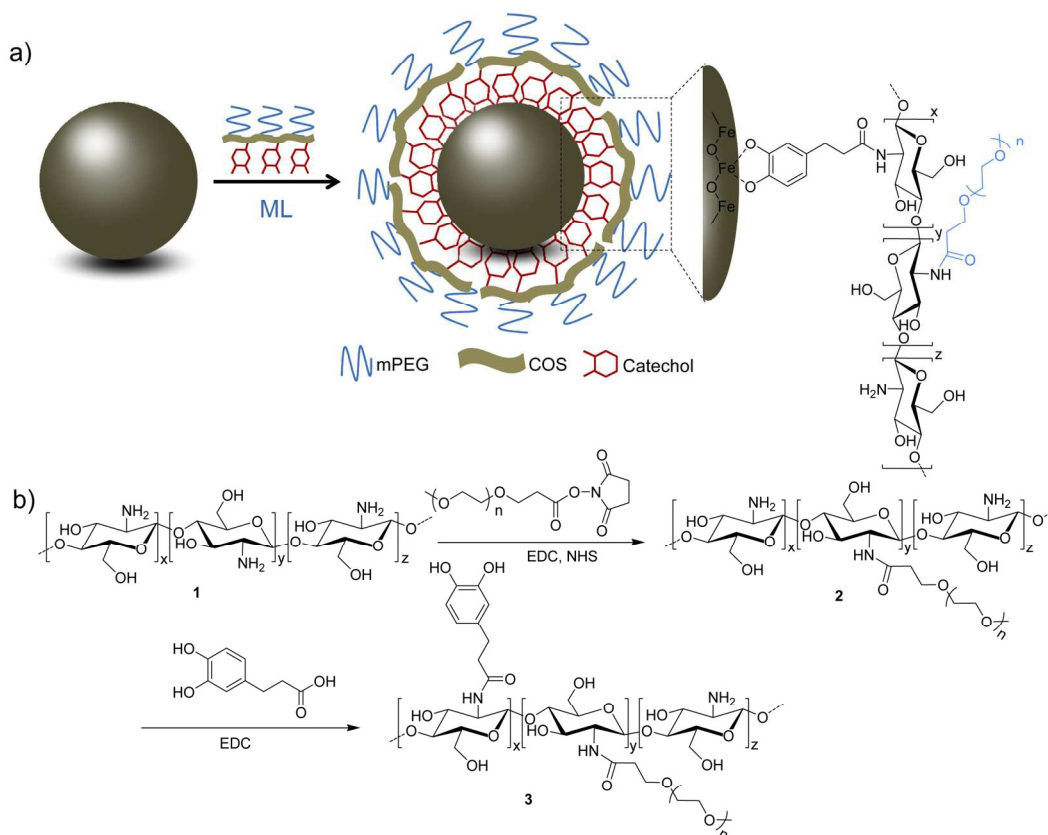
The 11 nm oleic acid-capped IONPs (OA-IONPs) were synthesized according to the reported methods.<sup>47</sup> Then, 10 mg of oleic acid-capped IONPs and 50 mg of ML were mixed in 10 mL of chloroform, and the resulting mixture was incubated for 1 h at room temperature. After the evaporation of the solvent, 5 mL of deionized water was added, and the resulting aqueous solution was filtered through a 200-nm syringe filter. To remove the excess ligand, the product was purified by spin filtration (Mw cutoff of 100 kDa, 5000×g, 10 min, Millipore).

### Surface functionalization of the ML-IONPs with fluorescein-isothiocyanate (FITC-IONPs)

The 1 mL of ML-stabilized IONPs (2 mg/mL in deionized water) was mixed with 10 μL of a FITC solution (10 mg/mL in DMSO), and incubated for 1 h at room temperature in the dark. The FITC-conjugated IONPs were purified by spin filtration (Mw cutoff of 100 kDa, 5000×g, 10 min, Millipore).

### *In vitro* cytotoxicity assay

RAW264.7 and HeLa cells were cultured in Dulbecco's modified eagle's medium supplemented with 10% (v/v) fetal bovine serum (BioWhittaker, Walkersville, MD, USA) and 1% penicillin/streptomycin (Gibco BRL, NY, USA) at 37°C in a humidified atmosphere containing 5% CO<sub>2</sub>. Cell viability was assessed using a 3-(4,5-dimethylthiazol-2-yl)-2,5-diphenyltetrazolium bromide (MTT) assay. The cells were seeded into 96-well plates for 24 h at a density of  $1 \times 10^4$  cells per well at 37°C in 5% CO<sub>2</sub> atmosphere. Samples at various concentrations were added to the cells and incubated for 48 h. The cells were washed twice with PBS and replenished with fresh medium. Subsequently, the cells were examined with a MTT assay.



**Scheme 1.** (a) Stabilization and functionalization of hydrophobic IONPs with a COS based multidentate ligand (ML). (b) Synthetic procedure for ML.

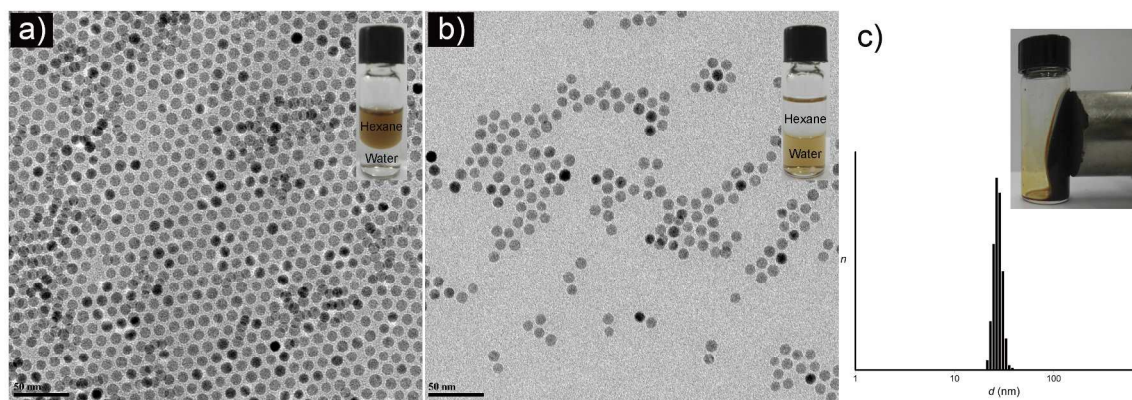


**Fig. 1** TEM images of (a) 11 nm hydrophobic IONPs and (b) hydrophilic counterparts that are stabilized with ML. (c) DLS data for the ML-stabilized IONPs and the inset displays a photograph of magnetically attracted IONPs dispersed in water with a high iron concentration (20 mg/mL). The scale bars correspond to 50 nm in the TEM images.

### Characterization techniques

<sup>1</sup>H NMR spectra were measured with a JEOL FT/NMR spectrometer. Fourier transformed infrared spectroscopy (FTIR) spectra were recorded on a Shimadzu IRPrestige-21 spectrometer with a resolution of 4 cm<sup>-1</sup>. Transmission electron microscopy (TEM) images were acquired using a Hitachi H7650 TEM operated at 100 kV. The hydrodynamic diameters (HDs) of nanoparticles was determined using a nanoparticle size analyzer (Sympatec GmbH, Germany) at 25 °C after the ML-stabilized

IONPs aqueous solutions were filtered through a 200-nm syringe filter. X-ray photoelectron spectroscopy (XPS) was performed on a laboratory-based spectrometer (K-alpha, Thermo) with photon energy of 1486.6 eV (Al K $\alpha$ ). Powder X-ray diffraction (XRD) patterns were measured using a diffractometer (Rigaku) with Cu K $\alpha$  radiation. Thermogravimetric analysis (TGA) of the dried sample was carried out on a TGA Q600 (TA instruments). The sample weight was monitored in the temperature range of 25 to 600°C with a heating rate of 10°C/min under air flow. The MR relaxivities of 11 nm ML-stabilized IONPs were measured using a 4.7 T clinical MRI instrument

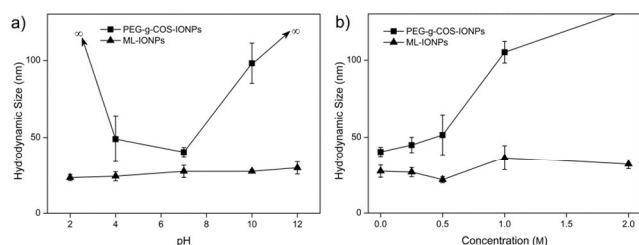


**Fig. 2** Stability tests of PEG-g-COS and ML stabilized IONPs as a function of (a) pH and (b) NaCl concentration.

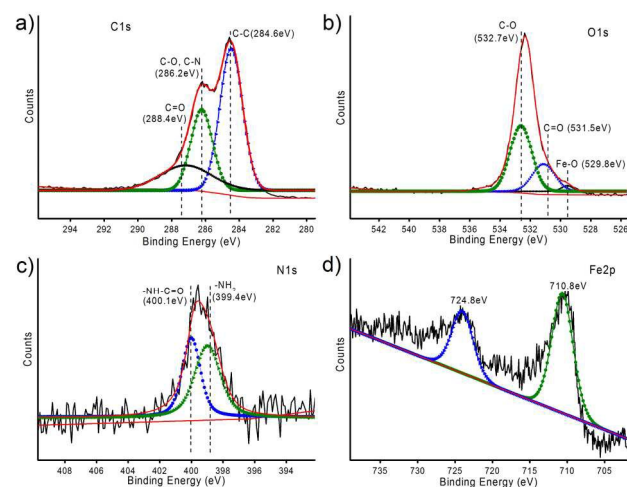


**Fig. 3** High-resolutions scan of the following regions: (a) C1s, (b) O1s, (c) N1s, and (d) Fe2p.

(Bruker BioSpec 47/40) with a head coil at the Korea Basic Science Institute in Ochang. An IR-FSE sequence was used to measure  $T_1$ , and its parameters were TR = 8000 ms and TE = 7.756 ms. A CPMG sequence was used to measure  $T_2$ , and its parameters were TR = 10000 ms and TE = 7.5 ms.

### *In vivo* MR imaging

For *in vivo* MR imaging, the animal protocol was approved by the Institutional Animal Care and Use Committee of the Wonkwang University. MR images of the mouse were obtained with a 4.7-T clinical MRI instrument (Bruker BioSpec 47/40) before and after the injection of 11 nm ML-stabilized IONPs (2.5 mg Fe/kg). The measurement parameters were as follows: flip angle = 90, TR = 3500 ms, TE = 12 ms, field of view = 50 × 50 mm, matrix = 256 × 256 mm, slice thickness = 1 mm, and NEX = 2.

## 15 Results and discussion

The ML described herein was synthesized *via* carbodiimide chemistry by forming an amide bond between a carboxylic acid group in hydrocaffeic acid and primary amine groups in mPEG-g-COS (Scheme 1). The degree of mPEG substitution in COS was controlled using a molar stoichiometric balance between mPEG and COS. Unlike the unmodified COS that is only water soluble, the mPEG-g-COS with a mPEG substitution degree of ~25% in the backbone was soluble in neutral, acidic and basic solutions, and organic solvents. The degree of mPEG substitution

was determined from the  $^1\text{H}$  NMR spectrum to be 25% by comparing the relative peak area of the methyl groups (3H,  $-\text{OCH}_3$ ,  $\delta$  3.33,  $\text{D}_2\text{O}$ ) of mPEG and the acetyl groups (3H,  $-\text{C}(\text{O})\text{CH}_3$ ,  $\delta$  2.01,  $\text{D}_2\text{O}$ ) on the COS backbone. Similarly, the degree of catechol substitution was controlled using a molar stoichiometric balance between hydrocaffeic acid and mPEG-g-COS, which was calculated to be 28% by comparing the relative peak area of the catechol groups (3H, aromatic ring proton,  $\delta$  6.5–6.8,  $\text{D}_2\text{O}$ ) and the acetyl groups on the COS backbone. The catechol content was also confirmed by the colorimetric assay ( $\lambda = 280$  nm, Figure S1).<sup>48–50</sup> The enhanced solubility of ML in the organic solvents is highly beneficial for stabilizing hydrophobic nanoparticles by ligand exchange. Additionally, catechol groups in ML mimicking a mussel adhesion mechanism. To demonstrate the ability of the ML for stabilization of IONPs, ML was directly used to modify 11 nm oleic acid-capped IONPs in chloroform by ligand exchange at room temperature. After the chloroform is removed by evaporation, the resulting hydrophilic IONPs are highly soluble in water, with a transfer yield of nearly 100%. The excess ligands in the hydrophilic IONPs solutions were removed by washing them through a spin filter three times (the detailed synthesis procedures and NMR of ML are shown in Scheme S1 and Figure S2).

TEM measurements show that the ML-stabilized hydrophilic IONPs have nearly identical sizes and shapes compared to their hydrophobic counterparts (Figure 1). Dynamic light scattering (DLS) results showed that ML-stabilized IONPs has uniform HDs of 26 nm, while that of the mPEG-g-COS stabilized IONPs increased to 41 nm. From TEM analysis, it was observed that ML-stabilized IONPs well dispersed as single particles (Figure 1b), but mPEG-g-COS stabilized IONPs became obvious aggregates (Figure S3). For the mPEG-g-COS-stabilized IONPs, it could be ascribed to the interaction of amine groups of COS with the IONPs surface resulted in crosslinking of the nanoparticles and induced aggregation of nanoparticle during the ligand exchange process. For the ML-stabilized IONPs, it was anticipated the catechol groups on the ML provide a strong interaction with the nanoparticle surface.<sup>51,52</sup> This indicates that ML can stabilize IONPs very well but mPEG-g-COS induced aggregation of nanoparticles, which is further consistent with the results from the following nanoparticles-stability measurements.

We investigated the stability of the resulting hydrophilic IONPs in various acidic, basic and salt solutions, for the evaluation of potential *in vivo* imaging applications. The results from stability tests show that mPEG-g-COS stabilized IONPs are unstable in strong acidic, basic, or concentrated NaCl solutions (Figure 2), whereas the ML-stabilized IONPs exhibited an excellent stability in NaCl solutions having concentrations up to 2 M and a very broad pH range of 1–12 (Figure 2). This effect may be attributable to the ability of ML to attach onto the IONPs surface through multiple attachments in a loops-and-trains conformation. In contrast to the standing “brush-like” conformations of single catechol-based ligands, it is believed that the linear multidentate ligand can cap nanoparticles in a loops-and-trains conformation, which can thus lead to enhanced colloidal stability of the modified nanoparticles.<sup>53</sup> This could be determined from the chain length of the COS molecule and the size of nanoparticles. The mean molecular weight of the

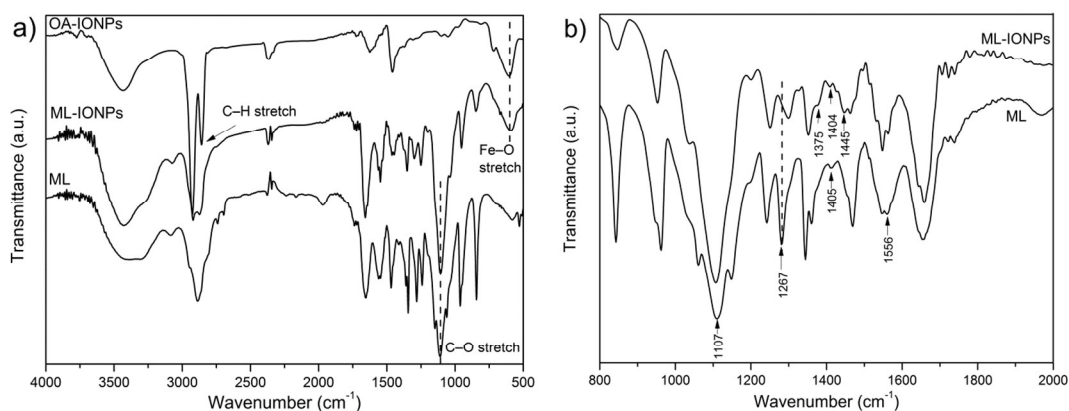


**Fig. 4** FTIR analysis of oleic acid-capped IONPs and hydrophilic counterparts that are stabilized with ML. FTIR absorption spectrum of ML is provided as a reference.

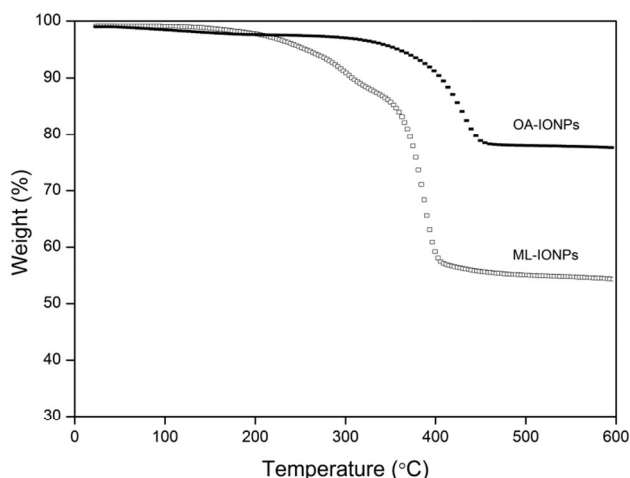


**Fig. 5** TGA curves of oleic acid-capped IONPs and hydrophilic counterparts that are stabilized with ML.

monomer units of COS was calculated to be 163.1 g/mol based on 92% deacetylation. Hence, the number of monomers in a COS (3 kDa) chain molecule is approximately 18. The virtual bond length per monomer unit of COS was reported to be 0.51 nm, regardless of the molecular weight, degree of deacetylation, and ionic strength.<sup>54</sup> Thus, the chain length of linear COS is 9.2 nm, which is possible to permit the linear ML to cap the surface of IONPs in a loops-and-trains conformation. ML-stabilized IONPs also showed great stability in PBS solution, suggesting that the adhesive properties of ML molecules bound on the IONPs were significantly maintained in aqueous physiological environment. X-ray diffraction (XRD) pattern was examined to confirm the crystal structure of ML-stabilized IONPs (Figure S4). The position and relative intensity of all diffraction peaks match well with those from the JDCPS card (19-0629) for magnetite, suggesting that the surface modification with ML did not induce any change on the crystallinity of the iron oxide core.

In order to confirm the existence of ML on IONPs surface, XPS and FTIR measurements were carried out. A typical survey spectrum of the ML-stabilized IONPs is presented in Figure 3. The high-resolution C1s spectrum displayed a broad shoulder between 282 and 290 eV. Taking bulk C1s at 284.6 eV as a standard, a broad shoulder can be fitted into three components on

the basis of the respective binding energies: carbon next to aromatic and aliphatic carbon (284.6 eV), carbon next to nitrogen or oxygen (286.2 eV), and the carbonyl carbon (288.4 eV). The O1s signal was also curve fitted into three components: oxygen of the metal oxide substrate (529.8 eV), carbonyl oxygen (531.5 eV), and oxygen next to aliphatic or aromatic carbon (532.7 eV). The N1s signal was fitted by two curves: one assigned to amine (399.4 eV) and one to the amide nitrogen (400.1 eV).<sup>55,56</sup> The binding energies of Fe 2p<sub>3/2</sub> and Fe 2p<sub>1/2</sub> appear at 710.8 and 724.8 eV and correspond to Fe–O bonds, which are typical of core level spectra of Fe<sub>3</sub>O<sub>4</sub>.<sup>57,58</sup> FTIR spectroscopy (Figure 4a) of the ML showed the expected signals associated with the PEG moieties and polysaccharide backbone<sup>45</sup> and the presence of the catecholic motif including the aryl (1405 cm<sup>-1</sup>) and phenolic alcohol bands (1267cm<sup>-1</sup>).<sup>45</sup> The FTIR spectrum (Figure 4a) of oleic acid-capped IONPs showed strong absorption bands at 2852 and 2923 cm<sup>-1</sup> that arose from symmetric and asymmetric C–H stretch in the oleyl chains, respectively.<sup>59</sup> The characteristic bands of oleic acid remarkably decreased after the ligand exchange, whereas new absorption bands centered at 1107 cm<sup>-1</sup> (C–O–C stretching) appeared to be related to PEG and the saccharine structure of COS. The FTIR spectral changes (Figure 4b) observed for the ML-stabilized IONPs confirming the formation of the Fe<sub>3</sub>O<sub>4</sub>-catechol coordination bond through loss of the phenolic band at 1267 cm<sup>-1</sup>.<sup>59</sup> The splitting of aryl vibrational bands into two signals further indicate that new coordination bond is formed, which commonly occurs when aryl groups are in close proximity to metals.<sup>45,60,61</sup> Raman spectroscopy of the ML-stabilized IONPs (Figure S5) also supports the presence of Fe<sub>3</sub>O<sub>4</sub>-catechol coordination bonds. The peaks at 540, 592, and 637 cm<sup>-1</sup> are assigned specifically to bidentate chelation of the metal ion by the phenolic oxygens of catecholic motif.<sup>45,62</sup> Taken together, it was evident that the oleic acid on the surface of magnetite nanoparticles was efficiently replaced by ML molecules. TGA was also performed to confirm the presence and amount of ML coating (Figure 5). The weight loss curve showed that the oleic acid-capped IONPs exhibited approximately 21% weight loss for hydrophobic surfactant layer, whereas ML-stabilized IONPs exhibited approximately 46% weight loss for ML shell. Therefore, the enhanced IONPs stability afforded by ML will greatly improve the performance of these nanoparticles in a variety of bio-applications where the ability to resist extreme pH and

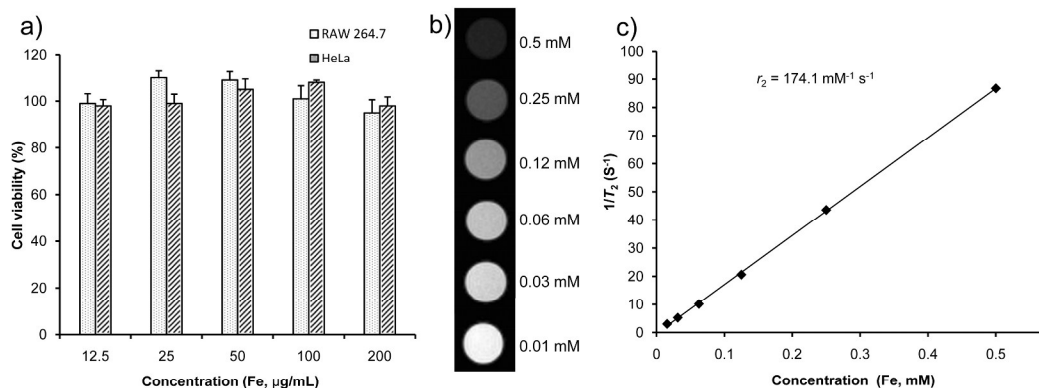


**Fig. 6** (a) Cytotoxicity of RAW 264.7 and HeLa cells evaluated by MTT assays after incubation with ML-stabilized IONPs with different Fe concentration for 48 h. (b)  $T_2$ -weighted MR images of ML-stabilized IONPs. (c) Plot of the inverse transverse relaxation times ( $1/T_2$ ) versus Fe concentration of ML-stabilized IONPs. The slope indicates the specific relaxivity value ( $r_2$ ).

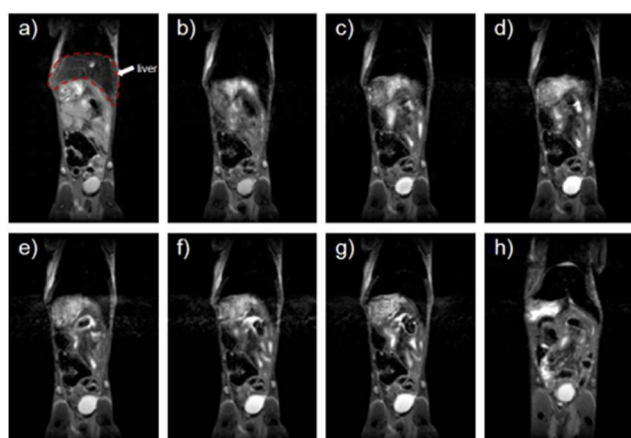


**Fig. 7** Time-dependent  $T_2$ -weighted MR images of a mouse: (a) before, (b) immediately after, (c) 10 min after, (d) 30 min after, (e) 1 h after, (f) 1.5 h after, (g) 2 h after, and (h) 24 h after intravenous administration of the 11 nm ML-stabilized IONPs.

concentrated salt solution is highly desirable. The remaining amine group was readily conjugated with other biomolecules through a mild EDC mediated coupling reaction. As an example, Figure S6 shows a photograph comparing the FITC-conjugated and un-conjugated ML-IONPs under UV illumination, indicating that FITC had been successfully grafted to the nanoparticles. This versatility is very useful for the introduction of a variety of functional groups and permits easy attachment of biomolecules.

The cytotoxicity of ML-stabilized IONPs was evaluated by MTT assay (Figure 6a). The results showed that cell viability was not reduced following culturing at different concentrations for 48 h after incubation. These results demonstrated that ML-stabilized IONPs are biocompatible. To validate the potential of ML-stabilized IONPs as a contrast agent, we acquired the spin-spin relaxation time ( $T_2$ )-weighted MR images and measured the relaxation rates as a function of metal concentration using a 4.7 T MRI scanner. As shown in the  $T_2$ -weighted images (Figure 6b), ML-stabilized IONPs displayed a significant signal reduction with increasing the particle concentration. The relaxivity value as high as  $174.10 \text{ mM}^{-1}\text{s}^{-1}$  for  $r_2$  and  $1.57 \text{ mM}^{-1}\text{s}^{-1}$  for  $r_1$  were obtained for ML-stabilized IONPs with a core diameter of 11 nm.

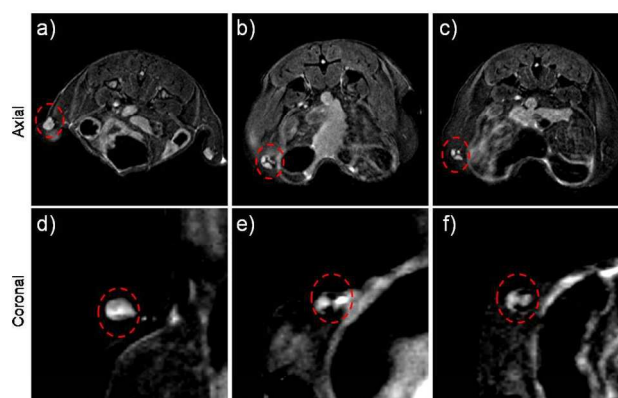


**Fig. 8** Time-dependent  $T_2$ -weighted MR images of lymph node acquired from a mouse: (a,d) before, (b,e) 10 h after, and (c,f) 24 h after injection of the 11 nm ML-stabilized IONPs.

It is well-known that the  $r_2/r_1$  ratio is an important parameter to estimate the efficiency of negative MRI contrast agents. In our study, the  $r_2/r_1$  ratio was calculated to be 110.9, which is significantly higher than the values for the commercial products, Feridex and Resovist,<sup>63,64</sup> thereby demonstrating that ML-stabilized IONPs could be efficient  $T_2$  contrast agents. These results indicate that ML promoted water dispersion without affecting the integrity or magnetic properties of the nanoparticles.

To demonstrate the suitability of using these water-soluble nanoparticles for biomedical diagnosis, we used ML-stabilized IONPs as a  $T_2$  contrast agent for enhanced MR imaging in a live animal model. The *in vivo* mouse MRI results obtained by using the ML-stabilized IONPs showed that the nanoparticles exhibited a long blood circulation time, as shown in the MR image obtained 24 h after injection (Figures 7). More importantly, when injected *via* the distal tail vein, the ML-stabilized IONPs successfully migrated from the injection site to the lymph nodes, resulting in a significant decrease in signal intensity (Figure 8, red dotted lines). However, there was no apparent contrast was detected from the lymph nodes containing only Feridex. We attribute this difference to the small HDs of ML-stabilized IONPs,<sup>65</sup> further demonstrating no aggregation and crosslinking of the nanoparticles. These data indicated that ML-stabilized IONPs are

highly stable in blood stream, presumably because PEG reduces undesirable non-specific cell interactions, prolongs plasma circulation.<sup>66</sup> Moreover, the mouse recovered from anesthesia spontaneously after the experiment and we did not observe adverse side effects on its behavior for more than a month after injection of the nanoparticles, which further suggests that the ML-stabilized IONPs are biocompatible and safe for *in vivo* application within a dosage range effective to provide MR contrast. The resultant ML-stabilized IONPs exhibited great stability in aqueous solutions with a wide range of pH and salt concentrations.

## Conclusions

In summary, we have demonstrated an approach of using a mussel-inspired PEGylated COS based ligand to convert hydrophobic IONPs into hydrophilic ones. The ML has been synthesized by modification of COS through a simple reaction sequence. The resultant ML-stabilized IONPs exhibited high stability in aqueous solutions with a wide range of pH and salt concentrations. Such stability is attributed to the surface modification through catechol domain. The ligand-exchange process was very simple and did not disturb the crystal structure, suggesting that the current strategy would afford stabilization and functionalization of various inorganic nanoparticles, which are poorly soluble and processable in aqueous solution. The successful *in vivo* MRI application of the ML-stabilized IONPs demonstrated their suitability for various nanoparticle-based biomedical applications.

## Acknowledgment

This work was supported by Wonkwang University (2014). C.L. acknowledge the NSFC (21401008).

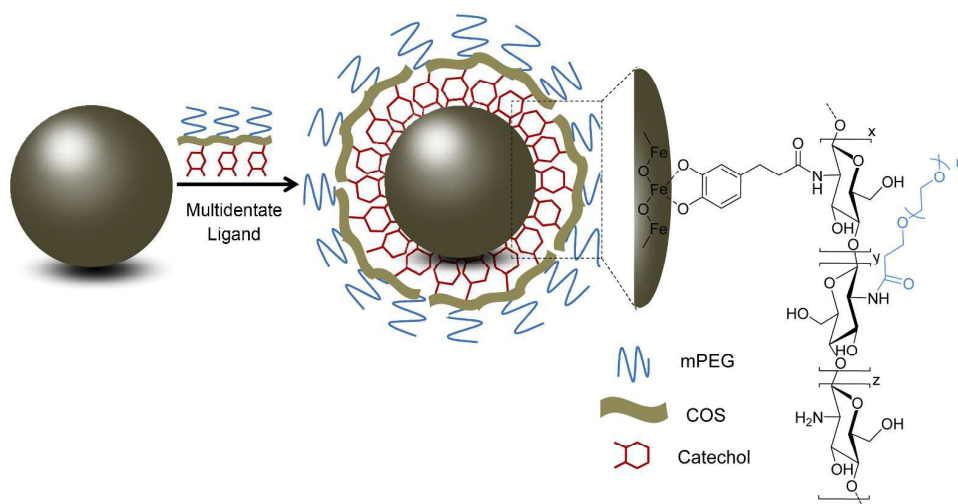
## Notes and references

- <sup>a</sup> Department of Chemistry, School of Science, Beijing Technology and Business University, Beijing 100048, P.R. China. Tel: +86 10 68985573; E-mail: luchichong@btbu.edu.cn
- <sup>b</sup> Department of Bionanochemistry, Wonkwang University, Iksan, Chonbuk 570-749, Republic of Korea. Fax: +82 63 8414893; Tel: +82 63 8506230; E-mail: geuyoon@wku.ac.kr
- <sup>c</sup> The High School Attached to Northwest Normal University, Lanzhou 730070, P.R. China
- <sup>†</sup> Electronic Supplementary Information (ESI) available: [The detailed synthesis procedures and NMR of ML, XRD, TEM, photographs, and MR images of stabilized IONPs.]. See DOI: 10.1039/b000000x/
- <sup>‡</sup> Footnotes should appear here. These might include comments relevant to but not central to the matter under discussion, limited experimental and spectral data, and crystallographic data.
- N. L. Rosi and C. A. Mirkin, *Chem. Rev.* 2005, **105**, 1547.
  - A. H. Lu, E. L. Salabas and F. Schüth, *Angew. Chem. Int. Ed.* 2007, **46**, 1222.
  - F. Hu, Y. S. Zhao, *Nanoscale*, 2012, **4**, 6235.
  - C.-M. J. Hu, R. H. Fang, B. T. Luk and L. Zhang, *Nanoscale*, 2014, **6**, 65.
  - E. Pösel, H. Kloust, U. Tromsdorf, M. Janschel, C. Hahn, C. Maßlo and H. Weller, *ACS Nano*, 2012, **6**, 1619.
  - Y. Jun, Y.-M. Huh, J. Choi, J.-H. Lee, H.-T. Song, S. Kim, S. Yoon, K.-S. Kim, J.-S. Shin, J.-S. Suh and J. Cheon, *J. Am. Chem. Soc.* 2005, **127**, 5732.
  - E. Amstad, M. Textor and E. Reimhult, *Nanoscale*, 2011, **3**, 2819.

- L. Wang, Q. Wu, S. Tang, J. Zeng, R. Qiao, P. Zhao, Y. Zhang, F. Hu, M. Gao, *RSC Adv.* 2013, **3**, 23454.
- H. B. Na, I. C. Song and T. Hyeon, *Adv. Mater.* 2009, **21**, 2133.
- M. Lattuada and T. A. Hatton, *Langmuir* 2007, **23**, 2158.
- R. Xie, U. Kolb, J. Li, T. Basché and A. Mews, *J. Am. Chem. Soc.* 2005, **127**, 7480.
- C. Lu, Z. Quan, J. C. Sur, S.-H. Kim, C. H. Lee and K. Y. Chai, *New J. Chem.* 2010, **34**, 2040.
- E. E. Lees, T.-L. Nguyen, A. H. A. Clayton and P. Mulvaney, *ACS Nano*, 2009, **3**, 1121.
- M. H. Stewart, K. Susumu, B. C. Mei, I. L. Medintz, J. B. Delehanty, J. B. Blanco-Canosa, P. E. Dawson and H. Mattoussi, *J. Am. Chem. Soc.* 2010, **132**, 9804.
- J. Xie, C. Xu, Z. Xu, Y. Hou, K. L. Young, S. X. Wang, N. Pourmand and S. Sun, *Chem. Mater.* 2006, **18**, 5401.
- H. Fan, E. W. Leve, C. Scullin, J. Gabaldon, D. Tallant, S. Bunge, T. Boyle, M. C. Wilson and C. J. Brinker, *Nano Lett.* 2005, **5**, 645.
- B. Dubertret, P. Skourides, D. J. Norris, V. Noireaux, A. H. Brivanlou and A. Libchaber, *Science* 2002, **298**, 1759.
- X. Wu, H. Liu, J. Liu, K. N. Haley, J. A. Treadway, J. P. Larson, N. Ge, F. Peale and M. P. Bruchez, *Nat. Biotechnol.* 2002, **21**, 41.
- W. W. Yu, E. Chang, J. C. Falkner, J. Zhang, A. M. Al-Somali, C. M. Sayes, J. Johns, R. Drezek and V. L. Colvin, *J. Am. Chem. Soc.* 2007, **129**, 2871.
- J. H. Waite, *J. Biol. Chem.* 1983, **258**, 2911.
- B. P. Lee, P. B. Messersmith, J. N. Israelachvili and J. H. Waite, *Annu. Rev. Mater. Res.* 2011, **41**, 99.
- H. Zhao, N. Robertson, S. A. Jewhurst and J. H. Waite, *J. Biol. Chem.* 2006, **281**, 11090.
- Q. Lin, D. Gourdon, C. Sun, N. Holten-Andersen, T. H. Anderson, J. H. Waite and J. N. Israelachvili, *PNAS* 2007, **104**, 3782.
- T. H. Anderson, J. Yu, A. Estrada, M. U. Hammer, J. H. Waite and J. N. Israelachvili, *Adv. Funct. Mater.* 2010, **20**, 4196.
- H. Lee, N. F. Scherer and P. B. Messersmith, *PNAS* 2006, **103**, 12999; H. Lee, S. M. Dellatore, W. M. Miller and P. B. Messersmith, *Science* 2007, **318**, 426.
- H. Lee, B. P. Lee and P. B. Messersmith, *Nature* 2007, **448**, 338.
- Y. Lee, H. Lee, Y. B. Kim, J. Kim, T. Hyeon, H. W. Park, P. B. Messersmith and T. G. Park, *Adv. Mater.* 2008, **20**, 4154.
- S. M. Kang, I. You, W. K. Cho, H. K. Shon, T. G. Lee, I. S. Choi, J. M. Karp and H. Lee, *Angew. Chem. Int. Ed.* 2010, **49**, 9401.
- M. I. Shukoor, F. Natalio, M. N. Tahir, M. Wiens, M. Tarantola, H. A. Therese, M. Barz, S. Weber, M. Terekhov, H. C. Schröder, W. E. G. Müller, A. Janshoff, P. Theato, R. Zentel, L. M. Schreiber and W. Tremel, *Adv. Funct. Mater.* 2009, **19**, 3717.
- D. Ling, W. Park, Y. I. Park, N. Lee, F. Li, C. Song, S. Yang, S. H. Choi, K. Na and T. Hyeon, *Angew. Chem. Int. Ed.* 2011, **50**, 11360.
- A. P. Zhu, N. Fang, M. B. Chan-Park, V. Chan, *Biomaterials* 2005, **26**, 6873.
- V. Belessi, R. Zboril, J. Tucek, M. Mashlan, V. Tzitzios and D. Petridis, *Chem. Mater.* 2008, **20**, 3298.
- A. Zhu, L. Yuan and T. Liao, *Int. J. Pharm.* 2008, **350**, 361; Z. Shi, K. G. Neoh, E. T. Kang, B. Shuter, S. Wang, C. Poh and W. Wang, *ACS Appl. Mater. Interfaces*, 2008, **1**, 328.
- Bhattacharya, M. Das, D. Mishra, I. Banerjee, S. K. Sahu, T. K. Maiti and P. Pramanik, *Nanoscale*, 2011, **3**, 1653.
- O. Veiseh, C. Sun, C. Fang, N. Bhattarai, J. Gunn, F. Kievit, K. Du, B. Pullar, D. Lee, R. G. Ellenbogen, J. Olson and M. Zhang, *Cancer Res.* 2009, **69**, 6200.
- S. H. Yuk, K. S. Oh, S. H. Cho, B. S. Lee, S. Y. Kim, B.-K. Kwak, K. Kim, I. C. Kwon, *Biomacromolecules*, 2011, **12**, 2335.
- A. López-Cruz, C. Barrera, V. L. Calero-DdelC and C. Rinaldi, *J. Mater. Chem.* 2009, **19**, 6870.
- K. H. Bae, M. Park, M. J. Do, N. Lee, J. H. Ryu, G. W. Kim, C. Kim, T. G. Park and T. Hyeon, *ACS Nano*, 2012, **6**, 5266.
- X. Liu, H. Huang, G. Liu, W. Zhou, Y. Chen, Q. Jin and J. Ji, *Nanoscale*, 2013, **5**, 3982.
- H. B. Na, G. Palui, J. T. Rosenberg, X. Ji, S. C. Grant and H. Mattoussi, *ACS Nano*, 2012, **6**, 389.
- W. Wang, X. Ji, H. B. Na, M. Safi, A. Smith, G. Palui, J. M. Perez and H. Mattoussi, *Langmuir* 2014, **30**, 6197.

- 42 M. I. Shukoor, F. Natalio, M. N. Tahir, M. Divekar, N. Metz, H. A. Therese, P. Theato, V. Ksenofontov, H. C. Schröder, W. E. G. Müller, W. Tremel, *J. Magn. Magn. Mater.* 2008, **320**, 2339.
- 43 X. Liu, J. Cao, H. Li, J. Li, Q. Jin, K. Ren and J. Ji, *ACS Nano*, 2013, **7**, 9384.
- 44 E. Amstad, T. Gillich, I. Bilecka, M. Textor and E. Reimhult, *Nano Lett.* 2009, **9**, 4042.
- 45 O. Zvarec, S. Purushotham, A. Masic, R. V. Ramanujan and A. Miserez, *Langmuir* 2013, **29**, 10899.
- 46 P. S. Yavvari and A. Srivastava, *J. Mater. Chem. B.* 2015, **3**, 899.
- 47 J. Park, K. An, Y. Hwang, J. G. Park, H. J. Noh, J. Y. Kim, J. H. Park, N. M. Hwang and T. Hyeon, *Nat. Mater.* 2004, **3**, 891.
- 48 L. E. Arnow, *J. Biol. Chem.* **1937**, 118, 531.
- 49 J. H. Waite and M. L. Tanzer, *Anal. Biochem.* **1981**, 111, 131.
- 50 D. W. Barnum, *Anal. Chim. Acta.* **1977**, 89, 157.
- 51 J. Xie, C. Xu, N. Kohler, Y. Hou and S. Sun, *Adv. Mater.* 2007, **19**, 3163.
- 52 C. Xu, K. Xu, H. Gu, R. Zheng, H. Liu, X. Zhang, Z. Guo and B. Xu, *J. Am. Chem. Soc.* 2004, **126**, 9938.
- 53 A. M. Smith and S. Nie, *J. Am. Chem. Soc.* 2008, **130**, 11278.
- 54 J. Cho, M.-C. Heuzey, A. Bégin and P. J. Carreau, *J. Food Eng.* 2006, **74**, 500.
- 55 X. G. Zhang, D. Y. Teng, Z. M. Wu, X. Wang, Z. Wang, D. M. Yu and C. X. Li, *J. Mater. Sci: Mater. Med.* 2008, **19**, 3525.
- 56 S. Zhang and K. E. Gonsalves, *Mater. Sci. Eng. C* 1995, **3**, 117.
- 57 J. S. Corneille, J.-W. He and D. W. Goodman, *Surf. Sci.* 1995, **338**, 211.
- 58 S. Lian, Z. Kang, E. Wang, M. Jiang, C. Hu and L. Xu, *Solid State Commun.* 2003, **127**, 605.
- 59 K. H. Bae, Y. B. Kim, Y. Lee, J. Y. Hwang, H. W. Park and T. G. Park, *Bioconjugate Chem.* 2010, **21**, 505.
- 60 M. J. Sever, J. T. Weisser, J. Monahan, S. Srinivasan and J. J. Wilker, *Angew. Chem., Int. Ed.* 2004, **43**, 448.
- 61 H. Gulley-Stahl, P. A. Hogan, W. L. Schmidt, S. J. Wall, A. Buhrlage and H. A. Bullen, *Environ. Sci. Technol.* 2010, **44**, 4116.
- 62 M. J. Harrington, A. Masic, N. Holten-Andersen, J. H. Waite and P. Fratzl, *Science* 2010, **328**, 216.
- 63 M. Rohrer, H. Bauer, J. Mintorovitch, M. Requardt and H. J. Weinmann, *Invest. Radiol.* 2005, **40**, 715.
- 64 J. Qin, S. Laurent, Y. S. Jo, A. Roch, M. Mikhaylova, Z. M. Bhujwalla, R. N. Muller and M. Muhammed, *Adv. Mater.* 2007, **19**, 1874.
- 65 C. Lu, L. R. Bhatt, H. Y. Jun, S. H. Park, K. Y. Chai, *J. Mater. Chem.* 2012, **22**, 19806.
- 66 N. F. Steinmetz, A. L. Ablack, J. L. Hickey, J. Ablack, B. Manocha, J. S. Mymryk, L. G. Luyt and J. D. Lewis, *Small*, 2011, **7**, 1664.

## Graphical Abstract



Mussel-inspired poly(ethylene glycol)-grafted-chitooligosaccharide based multidentate ligand (ML) is designed for preparing robust biocompatible magnetic iron oxide nanoparticles. The successful *in vivo* MRI application using ML-stabilized iron oxide nanoparticles confirmed their suitability for various biomedical applications.